# Global PDF-based Non-local Means Filtering of Resting fMRI Data

Jian Li[1], Soyoung Choi[1,2], Richard M. Leahy[1]

[1]Signal and Image Processing Institute, University of Southern California, Los Angeles, CA 90089
[2]Neuroscience Graduate Program, University of Southern California, Los Angeles, CA 90089

## Introduction

- Identification of brain networks from the temporal and spatial correlation patterns in resting fMRI (rfMRI) data [1] is challenging due to relatively small BOLD signal contrast and poor SNR.
- 3D Gaussian filtering or 2D Laplace-Betrami (LB) cortical surface filtering is commonly used to reduce noise. But this smoothing also mixes signals from spatially-adjacent functional regions, which in turn confounds delineation of the spatial boundaries of the regions that make up each network.
- Temporal non-local means (tNLM) filtering [2] resolves this issue using a non-local smoothing kernel, where the kernel weights are determined by a similarity measure between time series
- We developed tNLM-PDF, an extension of tNLM, that replaces a heuristically chosen filter kernel function with one based on an estimated probability density function representing connectivity between voxels.
- Cortical parcellation after tNLM-PDF filtering identifies interhemispheric networks which are constrained to one hemisphere using previous filtering methods

## Methods

- Surface-based tNLM-PDF filtering adopts tNLM's approach of filtering as a weighted average of signals, where the weights are based on temporal similarities between the rfMRI time series at the vertex being filtered and each of the other vertices in the surface tessellation.

$$s(i,t) = \sum_{j \neq i} s(j,t)\, w(i,j)$$

- Original tNLM filtering kernel has the weighting function

$$w(i,j) = e^{-\frac{2(1-r_{ij})}{h^2}}$$

where $r_{ij}$ is the Pearson correlation coefficient between time series at vertex $i$ and $j$.

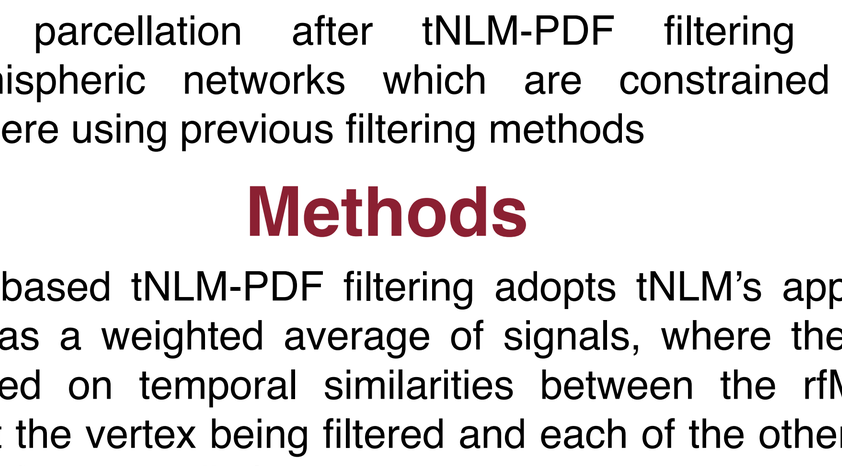


Figure 1: Estimated signal correlation distribution and the noise correlation distribution overlaid with tNLM kernel function as well as the tNLM-PDF kernel function.

- The tNLM-PDF differs from tNLM in two aspects:
  - The weighting kernel function is

$$w(i,j) = 1 - e^{-\frac{R(r)}{h^2}}$$

where $R(r) = P_S(r)/P_N(r)$ and $P_S(r)$ and $P_N(r)$ are the estimated pdfs of the Pearson correlation, using Gaussian mixture model, for within-network and between-network vertex pairs, respectively. The parameter $h$ controls the degree of smoothing and is chosen to maximally separate contributions from within and between networks while controlling the false positive rate to be not higher than $1e^{-4}$.

  - For each vertex, we compute $w(i,j)$ for the entire cerebral cortex, rather than using a restricted neighborhood as in tNLM [2].
- After filtering, the exponentially raised pair-wise correlation matrix was calculated as the edge weights which defines a connectivity graph.

$$A(i,j) = e^{r_{ij}}$$

- Then a normalized graph-cut (N-cuts) algorithm [3] was used to parcellate the brain into a set of 10 networks.

The tNLM-PDF filtering method will be available to the public in the future release of BrainSuite (www.brainsuite.org).

## Results & Discussion

Fig. 2 shows a comparison of unfiltered, LB, tNLM and tNLM-PDF filtered rfMRI data at two different time points for a single subject from the HCP dataset. Unfiltered data show the most spatial detail but also the largest amount of noise, while LB results show low noise characteristics but limited spatial complexity. tNLM and tNLM-PDF fall both between these extremes and exhibit the boundary-preserving properties that characterize NLM filtering. The two methods have similar spatial complexity but tNLM-PDF appears to detect regions which are more distinct by its sharper boundaries and increased cohesive signals.

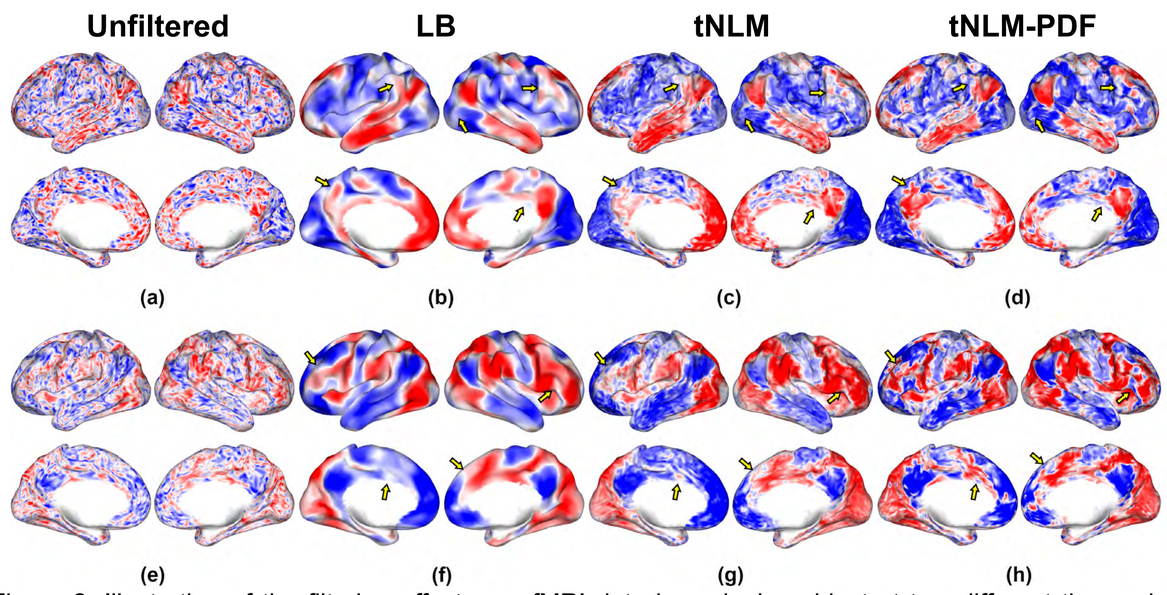


Figure 2: Illustration of the filtering effects on rfMRI data in a single subject at two different time points: 2'20'' for (a)-(d) and 2'54'' for (e)-(h). (a)(e) Unfiltered data (b)(f) Gaussian (LB) filtering (s=4) (c)(g) tNLM filtering (h=0.72) (d)(h) tNLM-PDF filtering. Color map ranges from -2 to 2 showing positive (red), negative (blue) and zero (white) BOLD signal strength.

To explore this further we parcellated the cortex into 10 networks and selected 4 sub-networks that delineate the default mode network (DMN) in Fig. 3. Top row shows the parcellation result where color is determined by the majority label across the 40 subjects with the opacity indicating the agreement level. Bottom row shows the labeling result from a single subject. With LB and tNLM filtering, the pink and yellow sub-networks seem to be homologous to one another, each constrained to one hemisphere. On the other hand, tNLM-PDF filtered data sub-delineates these larger regions into sub-networks which span across both hemispheres indicating interhemispheric functional correlation. In addition, some detailed spatial labeling patterns seen in tNLM-PDF filtering are absent from LB and tNLM filtering. Interestingly, these sub-delineations in tNLM-PDF filtered result, even from a individual rfMRI recording, are well aligned with those found in [4] (Fig. 3i), which were obtained through seed-based connectivity of 40 subjects. However, this can not be achieved using a single rfMRI dataset without tNLM-PDF filtering.

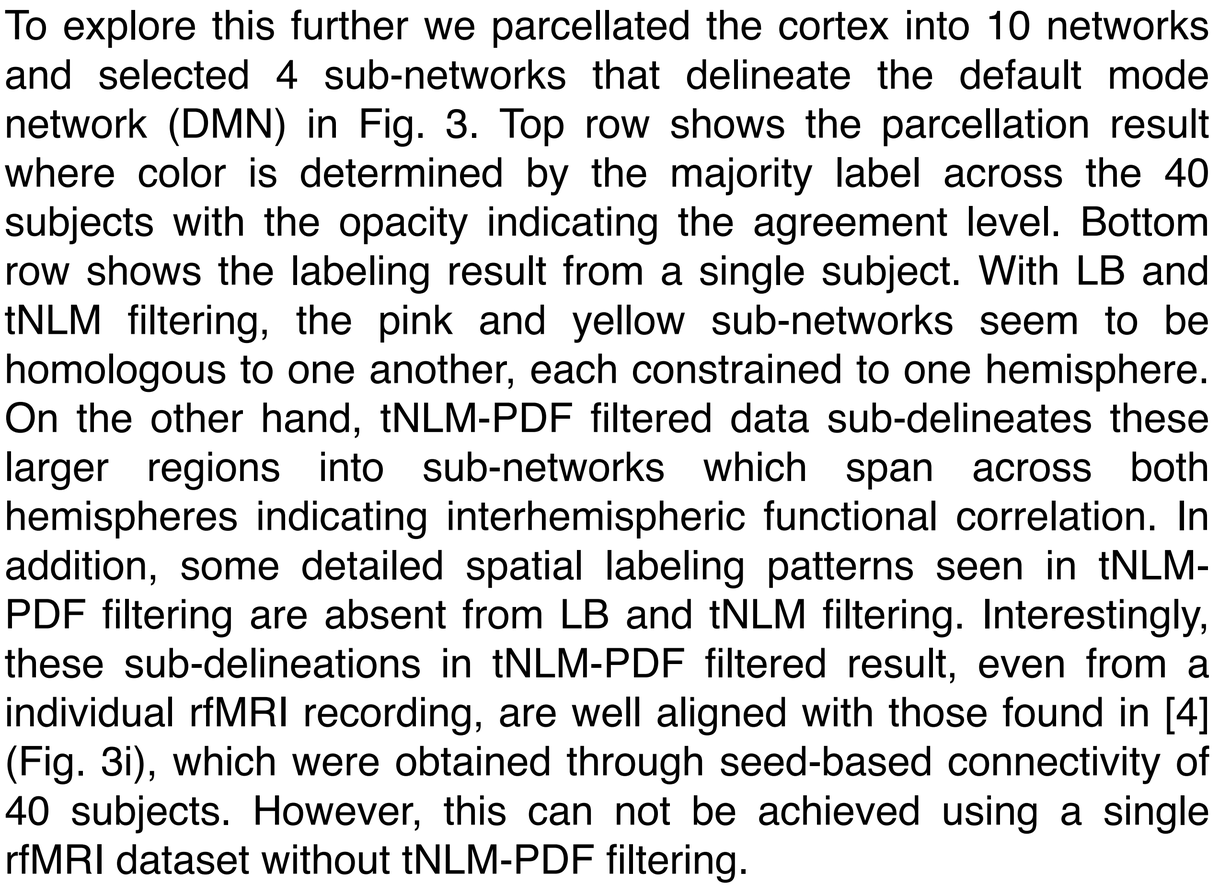


Figure 3: Cortical parcellations using N-cuts into 10 networks for (a)-(d) a group of 40 rfMRI sessions and (e)-(h) a single rfMRI session. Only the four subsetworks that collectively constitute the default mode network (DMN) are shown. (a)(e) Unfiltered data (b)(f) Gaussian (LB) filtering (s=4) (c)(g) tNLM filtering (h=0.72) (d)(h) tNLM-PDF filtering. and (i) Figure adapted from [4] that shows sub-delineation of DMN. Each distinct color represents one of the 4 clusters.

## Acknowledgment & References

This work was supported by NIH grants R01 NS089212 and R01 NS074980

[1] S. M. Smith, P. T. Fox, K. L. Miller, D. C. Glahn, P. M. Fox, C. E. Mackay, N. Filippini, K. E. Watkins, R. Toro, A. R. Laird and C. F. Beckmann (2009), "Correspondence of the brain's functional architecture during activation and rest," Proceedings of the National Academy of Sciences, vol. 106, no. 31, pp. 13040-13045.
[2] C. Bhushan, M. Chong, S. Choi, A. A. Joshi, J. P. Haldar, H. Damasio and R. M. Leahy (2016), "Temporal non-local means filtering reveals real-time whole-brain cortical interactions in resting fMRI," PloS one, vol. 11, no. 7, p. e0158504.
[3] J. Shi and J. Malik (2000), "Normalized cuts and image segmentation," IEEE Transactions on pattern analysis and machine intelligence, vol. 22, no. 8, pp. 888-905.
[4] R. L. Buckner, J. R. Andrews-Hanna and D. L. Schacter (2008), "The brain's default network," Annals of the New York Academy of Sciences, vol. 1124, no. 1, pp. 1-38.